

EXISTENCE OF SOLUTION TO A SYSTEM OF PDES MODELING THE CRYSTAL GROWTH INSIDE LITHIUM BATTERIES

ALEXANDROS SKOURAS, OMAR LAKKIS, AND VANESSA STYLES

ABSTRACT. We study a model for lithium (Li) electrodeposition on Li-metal electrodes that leads to dendritic pattern formation. The model comprises of a system of three coupled PDEs, taking the form of an Allen–Cahn equation, a Nernst–Planck equation and a Poisson equation. We prove existence of a weak solution and stability results for this system and present numerical simulations resulting from a finite element approximation of the system, which illustrate the dendritic nature of solutions to the model.

1. INTRODUCTION

In this paper we analyse a model for lithium (Li) electrodeposition on Li-metal electrodes in high-capacity lithium–oxygen and lithium–sulphur batteries. The model we consider is a variant of the thermodynamically consistent model introduced in Chen et al. [2015] to predict dendritic patterns which form during an electrochemical process using Li-electrodeposition. For ease of presentation we consider a simplified version in which, where possible, physical parameters have been set to 1:

$$\partial_t u = \nabla \cdot [\mathbf{A}(\nabla u)\nabla u] - g'(u) + m(c)h'(u) \quad \text{in } \Omega \times [0, T], \quad (1.1)$$

$$\partial_t c = \nabla \cdot [D(u)\nabla c + D_1(u, c)\nabla \phi] - \partial_t u \quad \text{in } \Omega \times [0, T], \quad (1.2)$$

$$\nabla \cdot [\sigma(u)\nabla \phi] = \partial_t u - \sigma'(u)\partial_x u \quad \text{in } \Omega \times [0, T], \quad (1.3)$$

together with appropriate boundary and initial data. Here c represents the ion concentration of Li^+ , ϕ denotes the electrostatic potential and u is a phase field variable that has a physical correspondence to the concentration of Li atoms. The specific forms of the anisotropic tensor $\mathbf{A}(u)$ and the functions $g(u)$, $m(c)$, etc. are defined in Section 2.1.

As humanity aims at reaching “net-zero” by 2050, replacing fossil fuels with renewable alternatives has spurred research in storage technologies, with lithium batteries being one of the favoured technologies. Electrodeposition in lithium batteries is an important phenomena that may lead to solid dendritic structures which, whilst remaining attached to the electrode, grow into the electrolyte solution. These structures can seriously compromise the performance and safety of such batteries, see for example Okajima et al. [2010], Akolkar [2013], Liang and Chen [2014], Chen et al. [2015], Yurkiv et al. [2018] and the references therein.

An early application of phase-field modelling to electrochemistry was introduced in Guyer et al. [2002] in which a new model was proposed and derived by a free energy functional that includes the electrostatic effect of charged particles leading to rich interactions between concentration, electrostatic potential and phase stability. This model was further studied by the same authors in Guyer et al. [2004b,a]. There is extensive literature on extensions of the model proposed in Guyer et al. [2002] to models taking similar forms to (1.1)–(1.3), namely a Nernst–Planck–Poisson system

coupled with an anisotropic phase-field equation, e.g. Okajima et al. [2010], Liang et al. [2012], Akolkar [2013], Chen et al. [2015], Yurkiv et al. [2018], Mu et al. [2019]. In these works numerical computations are presented that simulate the evolution of dendritic structures in Li-ion or Li-metal batteries. Works presenting numerical simulations of anisotropic phase field models go back many decades, see for example Kobayashi [1994], Karma and Rappel [1998], McFadden et al. [1993], Wheeler and McFadden [1996], Graser et al. [2013]. While mathematical analysis on the anisotropic phase-field model was developed in Elliott and Schätzle [1996, 1997], Taylor and Cahn [1998], Graser et al. [2013].

In this paper we adapt techniques from Burman and Rappaz [2003] in which the authors establish an existence result for weak solutions to a simplified version of the model (1.1) - (1.3). Specifically, the model studied in Burman and Rappaz [2003], which does not include an equation of type (1.3), is a system of two equations that take similar forms to (1.1) and (1.2). There are two key differences between the forms of (1.1) and (1.2) in this paper and their respective forms in Burman and Rappaz [2003], firstly, in this work the $\partial_t u$ term in (1.2) is not included in Burman and Rappaz [2003] and secondly, the $\nabla\phi$ advection term in (1.2) in this work is replaced by a ∇u advection term in Burman and Rappaz [2003].

The remainder of the paper is organised as follows. In Section 2 we present the full model together with a weak formulation, then we present the main result, which is an existence result, using Rothe's method, for solutions to the weak formulation. We prove the existence result by considering, in Section 3, a time discretization of the weak formulation and, in Section 4, taking the limit as the time step τ , of the discretization, tends to zero. We conclude with Section 5 in which we present a finite element discretisation of the model together with some numerical examples that illustrate the dendritic nature of solutions to the model.

We conclude this section with some comments on notation. We denote the L_2 -inner product on Ω by (\cdot, \cdot) and adopt the standard notation for Sobolev spaces, denoting the norm of $W_p^l(\Omega)$ ($l \in \mathbb{N}, p \in [1, \infty]$) by $\|\cdot\|_{l,p}$ and the semi-norm by $|\cdot|_{l,p}$. For $p = 2$, $W_2^l(\Omega)$ will be denoted by $H^l(\Omega)$ with the associated norm and semi-norm written, as respectively, $\|\cdot\|_l$ and $|\cdot|_l$. We denote the dual space of $H^1(\Omega)$ by $(H^1(\Omega))'$. In addition, we adopt the standard notation $W_p^l(a, b; X)$, ($l \in \mathbb{N}, p \in [1, \infty], (a, b)$ an interval in \mathbb{R}, X a Banach space) for time dependent spaces with norm $\|\cdot\|_{W_p^l(a,b;X)}$. Once again, we write $H^l(a, b; X)$ if $p = 2$. For a Hilbert Sobolev space with Dirichlet boundary condition on $\Sigma \subseteq \partial Q$ we write $H_{0|\Sigma}^m(Q)$ and $H_0^m(Q)$ if $\Sigma = \partial Q$. Lastly, C denotes a generic constant that may change from line to line.

2. WEAK FORMULATION OF THE MODEL

2.1. The model. The model, (1.1)–(1.3), takes the form of three interacting PDEs:

- (1.1) a nonlinear anisotropic Allen–Cahn type equation, for a phase-field variable u , with a forcing term, $m(c)h'(u)$, that accounts for the Butler–Volmer electrochemical reaction kinetics, which model the concentration of lithium atoms;
- (1.2) a reaction–diffusion Nernst–Planck type equation, which describes the dynamics of the concentration, c , of lithium ions;
- (1.3) a Poisson type equation that describes the electro static potential, ϕ , that drives the dynamics of the lithium ions.

For completeness we now rewrite the model together with the boundary and initial data:

$$\partial_t u = \nabla \cdot [\mathbf{A}(\nabla u)\nabla u] - g'(u) + m(c)h'(u) \quad \text{in } \Omega \times [0, T], \quad (2.1)$$

$$\partial_t c = \nabla \cdot [D(u)\nabla c + D_1(u, c)\nabla \phi] - \partial_t u \quad \text{in } \Omega \times [0, T], \quad (2.2)$$

$$\nabla \cdot [\sigma(u)\nabla \phi] = \partial_t u - \sigma'(u)\partial_x u \quad \text{in } \Omega \times [0, T], \quad (2.3)$$

$$\mathbf{A}(\nabla u)\nabla u \cdot \mathbf{n} = 0, \quad D(u)\nabla c \cdot \mathbf{n} = D_1(u, c)\nabla \phi \cdot \mathbf{n} \quad \text{on } \partial\Omega \times [0, T], \quad (2.4)$$

$$\sigma(u)\nabla \phi \cdot \mathbf{n} = 0 \text{ on } \Gamma_3 \times [0, T], \quad \phi = \phi_- \text{ on } \Gamma_1 \times [0, T], \quad \phi = 0 \text{ on } \Gamma_2 \times [0, T], \quad (2.5)$$

$$u(0) = u_0, \quad c(0) = c_0 \text{ in } \Omega. \quad (2.6)$$

Here $[0, T]$ is the time interval, the domain $\Omega = [0, L_1] \times [0, L_2]^{d-1} \subset \mathbb{R}^d$, $d = 2, 3$, is bounded and convex with Lipschitz boundary $\partial\Omega = \Gamma_1 \cup \Gamma_2 \cup \Gamma_3$, such that

$$\Gamma_1 := \{\mathbf{x} \in \partial\Omega : x_1 = 0\}, \quad \Gamma_2 := \{\mathbf{x} \in \partial\Omega : x_1 = L_1\} \quad \text{and} \quad \Gamma_3 = \partial\Omega \setminus (\Gamma_1 \cup \Gamma_2), \quad (2.7)$$

$$g(u) := u^2(1-u)^2/4, \quad h(u) := u^3(6u^2 - 15u + 10), \quad (2.8)$$

$$D(u) := D^e h(u) + D^s(1-h(u)), \quad \sigma(u) = \sigma^e h(u) + \sigma^s(1-h(u)), \quad \text{for } u \in \mathbb{R}, \quad (2.9)$$

$$m(c) := \begin{cases} C_1 - C_2, & c > 1, \\ C_1 - cC_2, & 0 \leq c \leq 1, \\ C_1, & c < 0, \end{cases} \quad D_1(u, c) := \begin{cases} D(u), & c > 1, \\ D(u)c, & 0 \leq c \leq 1, \\ 0, & c < 0, \end{cases} \quad (2.10)$$

with $D^e, D^s, \sigma^e, \sigma^s \in \mathbb{R}$ and $0 < D^s < D^e$, $0 < \sigma^e < \sigma^s$. The anisotropic diffusion tensor-valued field $\mathbf{A}(\mathbf{p})$ of $\mathbf{p} \in \mathbb{R}^d \setminus \{\mathbf{0}\}$ is defined in Section 2.4.

2.2. Remark (cut-off of constitutive functions). In Chen et al. [2015] the constitutive functions $D_1(u, c)$ and $m(c)$ are defined, for all $u, c \in \mathbb{R}$, to be $D_1(u, c) = D(u)c$ and $m(c) = C_1 - cC_2$ respectively. However to establish the analytical results in this paper, we consider their cut off variants defined in 2.10.

2.3. The weak formulation. A weak formulation of (2.1)-(2.6) is given as follows:

Let $u(0) = u_0 \in H^1(\Omega)$ and $c(0) = c_0 \in L_2(\Omega)$. Then, find (u, c, ϕ)

such that for all $(\chi, \eta) \in H^1(\Omega) \times H_0^1(\Gamma_1 \cup \Gamma_2)(\Omega)$,

$$(\partial_t u, \chi) + (\mathbf{A}(\nabla u)\nabla u, \nabla \chi) + (g'(u), \chi) = (m(c)h'(u), \chi), \quad (2.11a)$$

$$(\partial_t c, \chi) + (D(u)\nabla c, \nabla \chi) + (D_1(u, c)\nabla \phi, \nabla \chi) = (\partial_t u, \chi), \quad (2.11b)$$

$$(\sigma(u)\nabla \phi, \nabla \eta) = (-\partial_t u + \sigma'(u)\partial_x u, \eta), \quad (2.11c)$$

where

$$g'(s) = s(s-1)(s-\frac{1}{2}), \quad h'(s) = 30s^2(s-1)^2 \quad (2.12)$$

and

$$\sigma'(s) = 30(\sigma_e - \sigma_s)s^2(s-1)^2. \quad (2.13)$$

2.4. Anisotropic diffusion tensor. We define the tensor-valued field $\mathbf{A}(\mathbf{p})$, $\mathbf{p} \in \mathbb{R}^d \setminus \{\mathbf{0}\}$ in (1.1), which models the anisotropy of the growing crystals due to the cubic crystalline structure of lithium, by

$$\begin{aligned} \mathbf{A}(\mathbf{p}) &= a(\mathbf{p})\nabla a(\mathbf{p})\mathbf{p}^\top + a^2(\mathbf{p})\mathbf{I} \\ &= 16\delta a(\mathbf{p})|\mathbf{p}|^{-6} \left[p_i p_j (p_i^2 |\mathbf{p}|^2 - \sum_{k=1}^d p_k^4) \right]_{i=1, \dots, d}^{j=1, \dots, d} + a^2(\mathbf{p})\mathbf{I}, \end{aligned} \quad (2.14)$$

where

$$a(\mathbf{p}) = a_0(1 - 3\delta) \left(1 + \frac{4\delta}{1 - 3\delta} \frac{\sum_{j=1}^d p_j^4}{|\mathbf{p}|^4} \right), \quad (2.15)$$

for some material dependent parameters $a_0, \delta > 0$. Here $\mathbf{A}(\mathbf{p})$, $\mathbf{p} \in \mathbb{R}^d \setminus \{\mathbf{0}\}$ arises from the (Fréchet) derivative, J'_a , of the anisotropic Dirichlet energy,

$$J_a(w) := \frac{1}{2} \int_{\Omega} a^2(\nabla w) |\nabla w|^2 \quad (2.16)$$

such that $J'_a : H^1(\Omega) \rightarrow (H^1(\Omega))'$, $\forall v \in H^1(\Omega)$, satisfies

$$J'_a(w)[v] = \int_{\Omega} \mathbf{A}(\nabla w) \nabla w \cdot \nabla v, \quad \forall v \in H^1(\Omega). \quad (2.17)$$

2.5. Lemma (convexity of the anisotropic Dirichlet energy). *Recalling (2.15), for $\delta < 1/15$, the functional*

$$j_a(\mathbf{p}) := \frac{1}{2} \int_{\Omega} a^2(\mathbf{p}) |\mathbf{p}|^2 \quad (2.18)$$

is strictly convex in \mathbf{p} for all $\mathbf{p} \in (L_2(\Omega))^d$. It follows that the anisotropic Dirichlet energy $J_a(w)$ defined in (2.16) is strictly convex in $w \in H^1(\Omega)$.

Proof. The result is proved in Burman and Rappaz [2003] for $d = 2$. Here we extend it to the case $d = 3$. A sufficient condition for a functional to be strictly convex is the positivity of the Hessian matrix, Dacorogna [2008], i.e. we require

$$\mathcal{H}(\mathbf{p}) = \nabla^2 \bar{a}^2(\mathbf{p}) > 0, \quad \forall \mathbf{p} \in \text{Dom } \bar{a}^2,$$

where $\bar{a} : \mathbb{R}^d \rightarrow \mathbb{R}$ is given by

$$\bar{a}(\mathbf{p}) := \frac{\sqrt{2}a(\mathbf{p})}{2} |\mathbf{p}| \quad (2.19)$$

such that

$$j_a(\mathbf{p}) = \frac{1}{2} \int_{\Omega} a^2(\mathbf{p}) |\mathbf{p}|^2 = \int_{\Omega} \bar{a}^2(\mathbf{p}). \quad (2.20)$$

By Sylvester's criterion, a Hessian matrix is positive definite if all of the principal minors are positive. By symmetry in (p_1, p_2, p_3) , it is sufficient to check that $\mathcal{H}_{11}(\mathbf{p})$, the upper 2×2 matrix $\mathcal{H}_{1:2,1:2}(\mathbf{p})$ and $\mathcal{H}(\mathbf{p})$ itself have a positive determinant.

With the use of software Wolfram Mathematica Wolfram Research, Inc. [2024], our calculations show that \mathcal{H}_{11} is positive if and only if

$$\begin{aligned} 1 + 10\delta - 87\delta^2 > 0, \quad 1 + 6\delta - 27\delta^2 > 0, \quad 1 - 10\delta + 21\delta^2 > 0, \\ 1 - 14\delta - 15\delta^2 > 0, \quad 3 - 26\delta + 3\delta^2 > 0, \quad 5 + 22\delta - 15\delta^2 > 0. \end{aligned} \quad (2.21)$$

The above inequalities hold for $\delta < 1/15$, while the determinant of the upper 2×2 matrix is positive if and only if

$$1 - 15\delta > 0, \quad 1 + 6\delta - 315\delta^2 > 0, \quad 1 + 18\delta - 15\delta^2 > 0, \quad (2.22)$$

which are satisfied if and only if $\delta < 1/15$. Lastly, for the determinant of the Hessian matrix we have

$$\det(\mathcal{H}(\mathbf{p})) > 0 \Leftrightarrow 1 + 6\delta - 315\delta^2 > 0 \text{ and } 1 + 18\delta - 15\delta^2 > 0, \quad (2.23)$$

which also holds for $\delta < 1/15$.

The convexity of J_a follows from restricting j_a to the linear subspace of $L_2(\Omega)$ comprising all gradients of $H^1(\Omega)$ functions. \square

2.6. Remark (monotonicity). Since the anisotropic Dirichlet energy (2.16) is Fréchet differentiable and strictly convex it follows [from Pro 7.4 Showalter, 2013, e.g.] that the mapping $w \in H^1(\Omega) \mapsto J'_a(w) \in (H^1(\Omega))'$ is monotone and hemicontinuous. Thus we have

$$J_a(w) - J_a(v) \leq J'_a(w)[w - v] = \int_{\Omega} \mathbf{A}(\nabla w) \nabla w \nabla(w - v). \quad (2.24)$$

2.7. Remark (ellipticity). Noting Gräser [2011, Lem 2.2] we have that

$$(\mathbf{A}(\mathbf{p})\mathbf{p}, \mathbf{p}) = (\nabla(\bar{a}^2(\mathbf{p})), \mathbf{p}) = 2 \int_{\Omega} \bar{a}^2(\mathbf{p}), \quad \forall \mathbf{p} \in \mathbb{R}^d \quad (2.25)$$

thus from (2.15) and (2.19) we establish the bounds

$$c_A |w|_{\mathbf{H}^1(\Omega)}^2 \leq \int_{\Omega} \mathbf{A}(\nabla w) |\nabla w|^2 \leq C_A |w|_{\mathbf{H}^1(\Omega)}^2 \quad (2.26)$$

with

$$c_A := \min_{\mathbf{p} \in \mathbb{R}^d} a^2(\mathbf{p}) \quad \text{and} \quad C_A := \max_{\mathbf{p} \in \mathbb{R}^d} a^2(\mathbf{p}). \quad (2.27)$$

2.8. Theorem (existence of solutions). For $\delta < 1/15$, recall (2.15), initial data $(u_0, c_0) \in \mathbf{H}^1(\Omega) \times \mathbf{L}_2(\Omega)$ and $T > 0$, there exist

$$\begin{aligned} u &\in \mathbf{L}_2([0, T]; \mathbf{H}^1(\Omega)) \cap \mathbf{H}^1([0, T]; \mathbf{L}_2(\Omega)) \cap \mathbf{L}_{\infty}([0, T]; \mathbf{L}_{\infty}(\Omega)), \\ c &\in \mathbf{L}_2([0, T]; \mathbf{H}^1(\Omega)) \cap \mathbf{H}^1([0, T]; (\mathbf{H}^1(\Omega))') \cap \mathbf{L}_{\infty}([0, T]; \mathbf{L}_2(\Omega)) \end{aligned}$$

and

$$\phi \in \mathbf{L}_2([0, T]; \mathbf{H}_{0|\Gamma_1 \cup \Gamma_2}^1(\Omega))$$

such that (u, c, ϕ) satisfies $u(0) = u_0$, $c(0) = c_0$ and (2.11a)–(2.11c) for almost every $t \in [0, T]$ and every $(\chi, \eta) \in \mathbf{H}^1(\Omega) \times \mathbf{H}_{0|\Gamma_1 \cup \Gamma_2}^1(\Omega)$.

We split the proof of Theorem 2.8 in two parts. The first part, which is presented in Section 3, consists of proving existence of a solution to a semi-implicit Euler time discretization of (2.11a)–(2.11c) and deriving stability bounds on this solution. In the second part, presented in Section 4, we show that in the limit as the time step τ of the semi-discrete approximation tends to zero, there exists a solution that solves the weak formulation (2.11a)–(2.11c).

3. TIME DISCRETIZATION

In this section we consider a time discretization of (2.11a)–(2.11c). To this end, we partition the time interval $[0, T]$ into K equidistant steps, $0 = t_0 < t_1 < \dots < t_{K-1} < t_K = T$, so that for $k = 1, \dots, K$, $t_k = k\tau$.

We use the backward difference quotient, $d_{\tau} w^k = (w^k - w^{k-1})/\tau$ to obtain the following discretization of (2.11a)–(2.11c) in which we have linearized the convection term in (2.11b) and derived a specific form of the right hand side of (2.11a) that lends itself to proving the boundedness of u^k (see Lemma 3.2).

For all $(\chi, \eta) \in \mathbf{H}^1(\Omega) \times \mathbf{H}_{0|\Gamma_1 \cup \Gamma_2}^1(\Omega)$ and for all $k \geq 1, k \in \mathbb{N}$

$$\begin{aligned} (d_{\tau} u^k, \chi) + (\mathbf{A}(\nabla u^k) \nabla u^k, \nabla \chi) + (g'(u^k), \eta) &= ((m(c^{k-1}))^- h_1'(u^k), \chi) \\ &\quad + ((m(c^{k-1}))^+ h_2'(u^k), \chi), \end{aligned} \quad (3.1a)$$

$$(\sigma(u^k) \nabla \phi^k, \nabla \eta) = (-d_{\tau} u^k + \sigma'(u^k) \partial_x u^k, \eta), \quad (3.1b)$$

$$(d_{\tau} c^k, \chi) + (D(u^k) \nabla c^k, \nabla \chi) = -(d_{\tau} u^k, \chi) - (D_1(u^k, c^{k-1}) \nabla \phi^k, \nabla \chi), \quad (3.1c)$$

with $u^0 = u(0) = u_0$, $c^0 = c(0) = c_0$,

$$h_1'(u^k) := 30u^{k-1}u^k(u^k - 1)^2 \quad h_2'(u^k) := 30(u^k)^2(u^k - 1)(u^{k-1} - 1) \quad (3.2)$$

and $(\xi)^- := \min(0, \xi)$ and $(\xi)^+ := \max(0, \xi)$.

Note that the equations in the system (3.1a)–(3.1c) are not simultaneous, but will be solved in sequential order, first the phase-field equation (3.1a) is solved with given c^{k-1} to obtain u^k , then (3.1b) is solved with given u^k to obtain ϕ^k and finally the convection-diffusion equation (3.1c) is solved with given u^k and ϕ^k to obtain c^k .

We make the following assumptions on the time step τ , the anisotropy parameter δ , defined in (2.15), and the initial data u_0, c_0 ,

$$\begin{aligned} 0 < \tau < \min(1/2, 1/C^*, 1/4C^*), \\ \delta < 1/15, \\ 0 \leq u_0 \leq 1, u_0 \in H^1(\Omega), c_0 \in L_2(\Omega). \end{aligned} \quad (3.3)$$

Here C^* and C^* are defined by the bounds in (3.23) and (3.27) respectively.

3.1. Theorem (existence and uniqueness of a time-discrete solution). *Let assumptions (3.3) hold, then there exists a unique triple*

$$(u^k, c^k, \phi^k) \in (H^1(\Omega))^2 \times H_{0|\Gamma_1 \cup \Gamma_2}^1(\Omega), \quad (3.4)$$

with $k = 1, \dots, K = \lceil T/\tau \rceil$, satisfying the k -th step of (3.1a)–(3.1c).

We split the proof of Theorem 3.1 into several parts consisting of lemmas 3.4 – 3.7, in which we prove, in turn, the existence of unique solutions, u^k , ϕ^k and c^k to (3.1a), (3.1b) and (3.1c) respectively. In order to show the existence of a unique solution, u^k to (3.1a), we first show that u^k remains valued in $[0, 1]$ for all k .

3.2. Lemma (stability of the time-discrete order parameter). *Under assumptions (3.3) and $0 \leq u^{k-1} \leq 1$, we have*

$$0 \leq u^k \leq 1. \quad (3.5)$$

Proof. Setting $\chi = (u^k)^-$, in (3.1a) gives

$$\begin{aligned} (u^k, (u^k)^-) + \tau(\mathbf{A}(\nabla u^k) \nabla u^k, \nabla (u^k)^-) - \tau((m(c^{k-1}))^- h_1'(u^k), (u^k)^-) \\ - \tau((m(c^{k-1}))^+ h_2'(u^k), (u^k)^-) + \tau g'(u^k), (u^k)^-) = (u^{k-1}, (u^k)^-) \end{aligned} \quad (3.6)$$

then noting (2.26) we have

$$\begin{aligned} \|(u^k)^-\|_{L_2(\Omega)}^2 + \tau c_A |(u^k)^-|_{H^1(\Omega)}^2 \leq (u^{k-1}, (u^k)^-) + \tau((m(c^{k-1}))^- h_1'(u^k), (u^k)^-) \\ + \tau((m(c^{k-1}))^+ h_2'(u^k), (u^k)^-) - \tau(g'(u^k), (u^k)^-). \end{aligned} \quad (3.7)$$

By assumption $(u^{k-1})^- = 0$ and noting from (2.12) and (3.2) that $(g'(u^k), (u^k)^-) \geq 0$, $((m(c^{k-1}))^- h_1'(u^k), (u^k)^-) \leq 0$ and $((m(c^{k-1}))^+ h_2'(u^k), (u^k)^-) \leq 0$ it follows that

$$\|(u^k)^-\|_{L_2(\Omega)}^2 \leq 0 \Rightarrow u^k \geq 0. \quad (3.8)$$

Working similarly with $\eta = (u^k - 1)^+$ we obtain $u^k \leq 1$, which concludes the proof. \square

3.3. Remark (useful inequalities). Combining the result in Lemma 3.2 with (2.9), (2.10) and (2.12), we have

$$0 < \min(D^e, D^s) =: D_{\min} \leq D(u^k) \leq D_{\max} := \max(D^e, D^s), \quad (3.9)$$

$$0 < \min(\sigma^e, \sigma^s) =: \sigma_{\min} \leq \sigma(u^k) \leq \sigma_{\max} := \max(\sigma^e, \sigma^s), \quad (3.10)$$

$$|g'(u)| + |h'(u)| + |m(c)| + |D_1(u, c)| \leq C, \quad (3.11)$$

$$|(g'(u^k), \chi)| \leq C \|u^k\|_{L_2(\Omega)} \|\chi\|_{L_2(\Omega)}, \quad (3.12)$$

$$|((m(c^{k-1}))^- h_1'(u^k) + (m(c^{k-1}))^+ h_2'(u^k), \chi)| \leq C \|u^k\|_{L_2(\Omega)} \|\chi\|_{L_2(\Omega)}. \quad (3.13)$$

3.4. Lemma (existence and uniqueness of solutions for the time-discrete order parameter). *Suppose assumptions (3.3) hold and $u^{k-1} \in L_2(\Omega)$. Then there exists a unique solution $u^k \in H^1(\Omega)$ that satisfies the k -th step of (3.1a).*

Proof. We rewrite (3.1a) as follows

$$(d_\tau u^k, \chi) + I'(u^k)\chi = 0, \quad \forall \chi \in H^1(\Omega), \quad (3.14)$$

where $I' : H^1(\Omega) \rightarrow (H^1(\Omega))'$ is given by

$$I'(w)\chi = (\mathbf{A}(\nabla w)\nabla w, \nabla \chi) + (g'(w) - (m(c^{k-1}))^- h_1'(w) - (m(c^{k-1}))^+ h_2'(w), \chi) \quad (3.15)$$

is the (Fréchet) derivative of the energy functional $I : H^1(\Omega) \rightarrow \mathbb{R}$ with

$$I(w) = \int_\Omega \left(\frac{a(\nabla w)^2}{2} |\nabla w|^2 + g'(w) - (m(c^{k-1}))^- h_1'(w) - (m(c^{k-1}))^+ h_2'(w) \right). \quad (3.16)$$

We now seek a minimiser to the functional $I_k : H^1(\Omega) \rightarrow \mathbb{R}$

$$I_k(w) = \frac{1}{2\tau} \|w - u^{k-1}\|_{L_2(\Omega)}^2 + I(w), \quad (3.17)$$

which is the functional from which we derive (3.14). From Theorem 3.30 in Dacorogna [2008], to show the existence of a minimiser of (3.17) it is enough to prove that the function $F : \Omega \times \mathbb{R} \times \mathbb{R}^d \rightarrow \mathbb{R}$, defined by

$$F(x, \xi, \mathbf{p}) := \frac{a(\mathbf{p})^2}{2} |\mathbf{p}|^2 + \frac{1}{2\tau} (\xi - u^{k-1})^2 + g'(\xi) - (m(c^{k-1}))^- h_1'(\xi) - (m(c^{k-1}))^+ h_2'(\xi), \quad (3.18)$$

is a Carathéodory function, coercive and satisfies a sufficient growth condition. From [Bartels, 2015, Remark 2.4(i)] it follows that F is a Carathéodory function. From (3.11) we deduce that there are constants $\gamma_1, \gamma_2 > 0$ such that

$$-\gamma_1 \leq g'(\xi) - (m(c^{k-1}))^- h_1'(\xi) - (m(c^{k-1}))^+ h_2'(\xi) \leq \gamma_2. \quad (3.19)$$

Using (2.27) and (3.19) we establish the following bounds on F :

$$\begin{aligned} F(x, \xi, \mathbf{p}) &= \frac{a(\mathbf{p})^2}{2} |\mathbf{p}|^2 + \frac{1}{2\tau} (\xi - u^{k-1})^2 + g'(\xi) - (m(c^{k-1}))^- h_1'(\xi) \\ &\quad - (m(c^{k-1}))^+ h_2'(\xi) \\ &\geq \frac{c_A}{2} |\mathbf{p}|^2 + \frac{1}{4\tau} \xi^2 - \frac{1}{2\tau} (u^{k-1})^2 - \gamma_1 \end{aligned} \quad (3.20)$$

and

$$\begin{aligned} F(x, \xi, \mathbf{p}) &= \frac{a(\mathbf{p})^2}{2} |\mathbf{p}|^2 + \frac{1}{2\tau} (\xi - u^{k-1})^2 + g'(\xi) - (m(c^{k-1}))^- h_1'(\xi) \\ &\quad - (m(c^{k-1}))^+ h_2'(\xi) \\ &\leq \frac{C_A}{2} |\mathbf{p}|^2 + \frac{1}{\tau} \xi^2 + \frac{1}{\tau} (u^{k-1})^2 + \gamma_2. \end{aligned} \quad (3.21)$$

It only remains to show the uniqueness of the minimizer. Assume w_1 and w_2 are minimizers. From (3.14) it follows that

$$\begin{aligned} \int_\Omega \frac{1}{\tau} (w_1 - w_2)v + \int_\Omega (\mathbf{A}(\nabla w_1)\nabla w_1 - \mathbf{A}(\nabla w_2)\nabla w_2) \cdot \nabla v \\ + \int_\Omega (g'(w_1) - g'(w_2))v - \int_\Omega (m(c^{k-1}))^+ (h_1'(w_1) - h_1'(w_2))v \\ - \int_\Omega (m(c^{k-1}))^- (h_2'(w_1) - h_2'(w_2))v = 0. \end{aligned} \quad (3.22)$$

Choosing $v = w_1 - w_2$ in (3.22), using the Lipschitz continuity of g' , $h'_1(u^k)$ and $h'_2(u^k)$, (3.11), and noting from Remark 2.6 the monotonicity of the mapping $w \mapsto J'_a(w)$, we obtain

$$\begin{aligned} \frac{1}{\tau} \|w_1 - w_2\|_{L_2(\Omega)}^2 &\leq \int_{\Omega} |(g'(w_1) - g'(w_2))(w_1 - w_2)| \\ &+ C \int_{\Omega} |h'_1(w_1) - h'_1(w_2)| |w_1 - w_2| \leq C^* \|w_1 - w_2\|_{L_2(\Omega)}^2 \\ &+ C \int_{\Omega} |h'_2(w_1) - h'_2(w_2)| |w_1 - w_2| \leq C^* \|w_1 - w_2\|_{L_2(\Omega)}^2 \end{aligned} \quad (3.23)$$

and hence

$$\left(\frac{1}{\tau} - C^*\right) \|w_1 - w_2\|_{L_2(\Omega)}^2 \leq 0, \quad (3.24)$$

where C^* is independent of τ . Thanks to assumption (3.3) we have $\tau < 1/C^*$ and hence the uniqueness of the minimizer. \square

3.5. Lemma (energy estimates for the order parameter). *Under assumptions (3.3) we have*

$$\max_{l=0, \dots, K} \|u^l\|_{L_2(\Omega)}^2 + \tau \sum_{k=1}^K \|u^k\|_{H^1(\Omega)}^2 + \tau \sum_{k=1}^K \|d_{\tau} u^k\|_{L_2(\Omega)}^2 \leq C. \quad (3.25)$$

Proof. Setting $\chi = u^k$ in (3.14) and noting (2.26), (3.15), (3.13), (3.12) and

$$(d_{\tau} u^k, u^k) = \frac{\tau}{2} \|d_{\tau} u^k\|_{L_2(\Omega)}^2 + \frac{1}{2} d_{\tau} \|u^k\|_{L_2(\Omega)}^2 \quad (3.26)$$

we have

$$\begin{aligned} \frac{\tau}{2} \|d_{\tau} u^k\|_{L_2(\Omega)}^2 + \frac{1}{2} d_{\tau} \|u^k\|_{L_2(\Omega)}^2 + c_A |u^k|_{H^1(\Omega)}^2 &\leq |(g'(u^k), u^k)| \\ &+ |((m(c^{k-1}))^- h'_1(u^k), u^k)| + |((m(c^{k-1}))^+ h'_2(u^k), u^k)| \\ &\leq C^* \|u^k\|_{L_2(\Omega)}^2, \end{aligned} \quad (3.27)$$

where C^* is independent of τ . Multiplying by τ and summing from $k = 1, 2, \dots, l$, yields for any $l \leq K$ that

$$\left(\frac{1}{2} - \tau C^*\right) \|u^l\|_{L_2(\Omega)}^2 + \tau c_A \sum_{k=1}^l |u^k|_{H^1(\Omega)}^2 \leq \frac{1}{2} \|u^0\|_{L_2(\Omega)}^2 + \tau C \sum_{k=1}^{l-1} \|u^k\|_{L_2(\Omega)}^2. \quad (3.28)$$

Owing to (3.3) we have $\tau < 1/(4C^*)$ and hence using a generalized discretized Gronwall lemma, see [Bartels, 2015, Lem 2.2], we have that

$$\frac{1}{4} \max_{l=1, \dots, K} \|u^l\|_{L_2(\Omega)}^2 + \tau c_A \sum_{k=1}^K |u^k|_{H^1(\Omega)}^2 \leq \frac{1}{2} \|u^0\|_{L_2(\Omega)}^2 e^{CT} \leq C, \quad (3.29)$$

which yields the first two bounds in (3.25). To prove the third bound we set $\chi = d_{\tau} u^k$ in (3.14), multiply the resulting equation by τ and sum over $k = 1, 2, \dots, l$, to obtain for any $l \leq K$ that

$$\begin{aligned} \tau \sum_{k=1}^l \|d_{\tau} u^k\|_{L_2(\Omega)}^2 + \sum_{k=1}^l (\mathbf{A}(\nabla u^k) \nabla u^k, \nabla [u^k - u^{k-1}]) + \tau \sum_{k=1}^l (g'(u^k), d_{\tau} u^k) \\ = \tau \sum_{k=1}^l ((m(c^{k-1}))^- h'_1(u^k), d_{\tau} u^k) + \tau \sum_{k=1}^l ((m(c^{k-1}))^+ h'_2(u^k), d_{\tau} u^k). \end{aligned} \quad (3.30)$$

Using (2.24), (3.13) and (3.12) we have

$$\tau \sum_{k=1}^l \|d_\tau u^k\|_{L_2(\Omega)}^2 + \sum_{k=1}^l (J_a(u^k) - J_a(u^{k-1})) \leq C\tau \sum_{k=1}^l \|u^k\|_{L_2(\Omega)}^2 + \frac{\tau}{2} \sum_{k=1}^l \|d_\tau u^k\|_{L_2(\Omega)}^2. \quad (3.31)$$

Hence, noting (3.29), (3.3) and $u_0 \in H^1(\Omega)$, we have

$$\frac{\tau}{2} \sum_{k=1}^l \|d_\tau u^k\|_{L_2(\Omega)}^2 + J_a(u^l) \leq J_a(u^0) + \frac{\tau C}{4} \sum_{k=1}^l \|u^k\|_{L_2(\Omega)}^2 \leq C, \quad (3.32)$$

which completes the proof. \square

3.6. Lemma (existence and uniqueness of the time-discrete potential). *Let assumptions (3.3) hold. Then there exists a unique solution $\phi^k \in H_{0|\Gamma_1 \cup \Gamma_2}^1(\Omega)$, that satisfies the k -th step of (3.1b).*

Proof. We introduce the form $b_1 : (H^1(\Omega))^2 \rightarrow \mathbb{R}$

$$b_1(u^k; v, w) = \int_{\Omega} \sigma(u^k) \nabla v \cdot \nabla w, \quad (3.33)$$

which is bilinear in respect to v and w . Using (3.33) we can rewrite (3.1b) as

$$b_1(u^k; \phi^k, \eta) = -(d_\tau u^k + \sigma'(u^k) \partial_x u^k, \eta). \quad (3.34)$$

We now prove existence of a weak solution using the Lax–Milgram Theorem. The coercivity and boundedness of b_1 follow from (3.10) and the equivalence of the H^1 semi-norm and the H^1 norm under a homogeneous Dirichlet boundary condition:

$$b_1(u^k; v, v) = \int_{\Omega} \sigma(u^k) |\nabla v|^2 \geq \sigma_{\min} |v|_{H^1(\Omega)}^2, \quad (3.35)$$

$$|b_1(u^k; v, w)| \leq \sigma_{\max} |v|_{H^1(\Omega)} |w|_{H^1(\Omega)}. \quad (3.36)$$

From Lemma 3.5 we have that

$$\|u^k\|_{H^1(\Omega)}^2 + \|d_\tau u^k\|_{L_2(\Omega)}^2 \leq \frac{C}{\tau} \quad (3.37)$$

which together with (2.13), imply

$$\|d_\tau u^k + \sigma'(u^k) \partial_x u^k\|_{L_2(\Omega)}^2 \leq \frac{C}{\tau}. \quad (3.38)$$

Thus, by the Lax–Milgram Theorem, (3.1b) has a unique solution at the k -th step $\phi^k \in H_{0|\Gamma_1 \cup \Gamma_2}^1(\Omega)$, with

$$\|\phi^k\|_{H^1(\Omega)} \leq \frac{C}{\tau}. \quad (3.39)$$

\square

3.7. Lemma (existence and uniqueness of the time-discrete concentration). *Under assumptions (3.3), if $\|c^{k-1}\|_{L_2(\Omega)} \leq C$, then there exists a unique solution $c^k \in H^1(\Omega)$ that satisfies the k -th step of (3.1c).*

Proof. We introduce the form $b_2 : (H^1(\Omega))^2 \rightarrow \mathbb{R}$

$$b_2(u^k; w, v) := \int_{\Omega} D(u^k) \nabla w \cdot \nabla v + \frac{1}{\tau} wv, \quad (3.40)$$

which is bilinear for w and v . Using (3.40) we can rewrite (3.1c) as

$$b_2(u^k; c^k, \chi) = -(d_\tau u^k, \chi) - (D_1(u^k, c^{k-1}) \nabla \phi^k, \nabla \chi) + \frac{1}{\tau} (c^{k-1}, \chi). \quad (3.41)$$

Again we prove existence of a weak solution using the Lax–Milgram Theorem. Coercivity and boundedness of b_2 follow from (3.9):

$$\begin{aligned} b_2(u^k; w, w) &= \int_{\Omega} D(u^k) |\nabla w|^2 + \frac{1}{\tau} |w|^2 \geq D_{\min} |w|_{\mathbf{H}^1(\Omega)}^2 + \frac{1}{\tau} \|w\|_{L_2(\Omega)}^2 \\ &\geq D_{\min} \|w\|_{\mathbf{H}^1(\Omega)}^2, \end{aligned} \quad (3.42)$$

$$\begin{aligned} |b_2(u^k; w, v)| &= \left| \int_{\Omega} D(u^k) \nabla w \cdot \nabla v + \frac{1}{\tau} wv \right| \leq \int_{\Omega} |D(u^k)| |\nabla w| |\nabla v| + \frac{1}{\tau} |w| |v| \\ &\leq D_{\max} |w|_{\mathbf{H}^1(\Omega)} |v|_{\mathbf{H}^1(\Omega)} + \frac{1}{\tau} \|w\|_{L_2(\Omega)} \|v\|_{L_2(\Omega)} \leq \frac{1}{\tau} \|w\|_{\mathbf{H}^1(\Omega)} \|v\|_{\mathbf{H}^1(\Omega)}. \end{aligned} \quad (3.43)$$

From Lemma 3.5, the assumption that $\|c^{k-1}\|_{L_2(\Omega)} \leq C$, (3.11) and (3.39) we have

$$\|d_{\tau} u^k\|_{L_2(\Omega)} + \frac{1}{\tau} \|c^{k-1}\|_{L_2(\Omega)} + \|D_1(u^k, c^{k-1}) \nabla \phi^k\|_{L_2(\Omega)}^2 \leq \frac{C}{\tau}. \quad (3.44)$$

Thus the right hand side of (3.41) is bounded, dependent on τ , in $(\mathbf{H}^1(\Omega))'$ and by the Lax–Milgram Theorem, there exists a unique solution $c^k \in \mathbf{H}^1(\Omega)$ that satisfies the k -th step of (3.1c). \square

3.8. Lemma (energy stability of the potential). *Let assumptions (3.3) hold and let ϕ^k , be the solution to the k -th step of (3.1b). Then we have*

$$\tau \sum_{k=1}^K \|\phi^k\|_{\mathbf{H}^1(\Omega)}^2 \leq C. \quad (3.45)$$

Proof. We set $\eta = \phi^k$ in (3.1b) to give

$$\int_{\Omega} \sigma(u^k) |\nabla \phi^k|^2 = - \int_{\Omega} d_{\tau} u^k \phi^k + \int_{\Omega} \sigma'(u^k) \partial_x u^k \phi^k.$$

Noting (3.10) we have

$$\sigma_{\min} |\phi^k|_{\mathbf{H}^1(\Omega)}^2 \leq \|d_{\tau} u^k\|_{L_2(\Omega)} \|\phi^k\|_{L_2(\Omega)} + \sigma'_{\max} \|\partial_x u^k\|_{L_2(\Omega)} \|\phi^k\|_{L_2(\Omega)}, \quad (3.46)$$

where $\sigma'_{\max} := \max_{s \in \mathbb{R}} \sigma'(s)$. Hence from the Friedrichs inequality we have

$$\begin{aligned} \frac{\sigma_{\min}}{2C_f} \|\phi^k\|_{L_2(\Omega)}^2 + \frac{\sigma_{\min}}{2} |\phi^k|_{\mathbf{H}^1(\Omega)}^2 &\leq C \|d_{\tau} u^k\|_{L_2(\Omega)}^2 + \frac{\sigma_{\min}}{8C_f} \|\phi^k\|_{L_2(\Omega)}^2 \\ &\quad + C \|\partial_x u^k\|_{L_2(\Omega)}^2 + \frac{\sigma_{\min}}{8C_f} \|\phi^k\|_{L_2(\Omega)}^2 \end{aligned} \quad (3.47)$$

where C_f is the constant in the Friedrichs inequality, which is associated with the diameter of Ω . After rearranging (3.47), multiplying the resulting inequality by τ and summing over $k = 1, 2, \dots, l$, for any $l \leq K$ we have

$$\tau \sum_{k=1}^l \|\phi^k\|_{\mathbf{H}^1(\Omega)}^2 \leq C \left(\tau \sum_{k=1}^l \|d_{\tau} u^k\|_{L_2(\Omega)}^2 + \tau \sum_{k=1}^l \|\partial_x u^k\|_{L_2(\Omega)}^2 \right) \quad (3.48)$$

and the result follows from Lemma 3.5. \square

3.9. Lemma (energy estimates for the concentration). *Let assumptions (3.3) hold. Then*

$$\max_{l=0, \dots, K} \|c^l\|_{L_2(\Omega)}^2 + \tau \sum_{k=1}^K \|c^k\|_{\mathbf{H}^1(\Omega)}^2 + \tau \sum_{k=1}^K \|d_{\tau} c^k\|_{(\mathbf{H}^1(\Omega))'}^2 \leq C. \quad (3.49)$$

Proof. Setting $\chi = c^k$ in (3.1c) gives

$$(d_\tau c^k, c^k) + (D(u^k) \nabla c^k, \nabla c^k) = -(d_\tau u^k, c^k) - (D_1(u^k, c^{k-1}) \nabla \phi^k, \nabla c^k) \quad (3.50)$$

and noting (3.26), (3.9) and (3.11), we obtain

$$\begin{aligned} \frac{\tau}{2} \|d_\tau c^k\|_{L_2(\Omega)}^2 + \frac{1}{2} d_\tau \|c^k\|_{L_2(\Omega)}^2 + D_{\min} |c^k|_{H^1(\Omega)}^2 &\leq \frac{1}{2} \|d_\tau u^k\|_{L_2(\Omega)}^2 + \frac{1}{2} \|c^k\|_{L_2(\Omega)}^2 \\ &+ C |\phi^k|_{H^1(\Omega)}^2 + \frac{D_{\min}}{2} |c^k|_{H^1(\Omega)}^2. \end{aligned} \quad (3.51)$$

After rearranging (3.51), multiplying the resulting inequality by τ and summing over $k = 1, 2, \dots, l$, for any $l \leq K$, we have

$$\begin{aligned} \frac{\tau^2}{2} \sum_{k=1}^l \|d_\tau c^k\|_{L_2(\Omega)}^2 + \frac{1}{2} \|c^l\|_{L_2(\Omega)}^2 + \tau \frac{D_{\min}}{2} \sum_{k=1}^l |c^k|_{H^1(\Omega)}^2 \\ \leq \frac{1}{2} \|c^0\|_{L_2(\Omega)}^2 + \frac{\tau}{2} \sum_{k=1}^l \|d_\tau u^k\|_{L_2(\Omega)}^2 + \frac{\tau}{2} \sum_{k=1}^l \|c^k\|_{L_2(\Omega)}^2 + \tau C \sum_{k=1}^l |\phi^k|_{H^1(\Omega)}^2. \end{aligned}$$

Thus, noting from assumption (3.3) that $c_0 \in L_2(\Omega)$, we have

$$\begin{aligned} \frac{1}{2} (1 - \tau) \|c^l\|_{L_2(\Omega)}^2 + \tau \frac{D_{\min}}{2} \sum_{k=1}^l |c^k|_{H^1(\Omega)}^2 &\leq C \left(1 + \tau \sum_{k=1}^l \|d_\tau u^k\|_{L_2(\Omega)}^2 \right. \\ &\left. + \tau \sum_{k=1}^l |\phi^k|_{H^1(\Omega)}^2 + \tau \sum_{k=1}^{l-1} \|c^k\|_{L_2(\Omega)}^2 \right). \end{aligned} \quad (3.52)$$

Since (3.3) holds we have $\tau < 1/2$ and hence using the discrete Gronwall Lemma, we obtain

$$\begin{aligned} \frac{1}{4} \max_{l=1, \dots, K} \|c^l\|_{L_2(\Omega)}^2 + \tau \frac{D_{\min}}{2} \sum_{k=1}^K |c^k|_{H^1(\Omega)}^2 \\ \leq C \left(1 + \tau \sum_{k=1}^K \|d_\tau u^k\|_{L_2(\Omega)}^2 + \tau \sum_{k=1}^K |\phi^k|_{H^1(\Omega)}^2 \right) e^{\frac{\tau}{2}} \end{aligned} \quad (3.53)$$

and from lemmas 3.5 and 3.8 we conclude

$$\frac{1}{4} \max_{l=0, \dots, K} \|c^l\|_{L_2(\Omega)}^2 + \tau \sum_{k=1}^K |c^k|_{H^1(\Omega)}^2 \leq C. \quad (3.54)$$

To prove the last estimate in (3.49), we note from (3.1c), (3.9) and (3.11) that

$$\begin{aligned} (d_\tau c^k, \chi)_{((H^1(\Omega))', H^1(\Omega))} &\leq \|D(u^k) \nabla c^k\|_{L_2(\Omega)} \|\nabla \chi\|_{L_2(\Omega)} + \|d_\tau u^k\|_{L_2(\Omega)} \|\chi\|_{L_2(\Omega)} \\ &+ \|D_1(u^k, c^{k-1}) \nabla \phi^k\|_{L_2(\Omega)} \|\nabla \chi\|_{L_2(\Omega)} \\ &\leq C (|c^k|_{H^1(\Omega)} + |\phi^k|_{H^1(\Omega)} + \|d_\tau u^k\|_{L_2(\Omega)}) \|\chi\|_{H^1(\Omega)} \end{aligned} \quad (3.55)$$

and so we conclude

$$\|d_\tau c^k\|_{(H^1(\Omega))'}^2 \leq C (|c^k|_{H^1(\Omega)}^2 + |\phi^k|_{H^1(\Omega)}^2 + \|d_\tau u^k\|_{L_2(\Omega)}^2). \quad (3.56)$$

The required result follows after multiplying by τ , summing over $k = 1, 2, \dots, K$ and noting (3.54) and lemmas 3.5 and 3.8. \square

Proof of Theorem 3.1. Theorem 3.1 is a direct consequence of lemmas 3.4, 3.6 and 3.7. \square

4. WEAK CONVERGENCE OF THE LIMITS

In this section, we prove that as $\tau \rightarrow 0$ subsequences of the solution to (3.1a)–(3.1c) converge to a solution of (2.11a)–(2.11c).

Introduce the notation

$$u_\tau^-(t) = u^{k-1}, \quad u_\tau^+(t) = u^k \text{ for } t_{k-1} < t \leq t_k, \quad (4.1)$$

and do the same $c_\tau^\pm(t), \hat{c}_\tau(t), \phi_\tau^\pm(t), \hat{\phi}_\tau(t)$. Also use u_τ to denote the interpolate

$$\hat{u}_\tau(t) = \frac{t - t_{k-1}}{\tau} u^k + \frac{t_k - t}{\tau} u^{k-1}, \text{ for } t_{k-1} \leq t \leq t_k, k = 0, \dots, K. \quad (4.2)$$

Next recalling (3.2), the terms on the left hand side of (3.1a) can be reformulated as

$$\begin{aligned} ((m(c^{k-1}))^- h_1'(u^k), \chi) + ((m(c^{k-1}))^+ h_2'(u^k), \chi) &= 30 (m(c^{k-1}) u^{k-1} u^k (u^k - 1)^2, \chi) \\ &\quad + 30 ((m(c^{k-1}))^+ (u^k - 1) u^k (u^{k-1} - u^k), \chi). \end{aligned} \quad (4.3)$$

Thus rewriting (3.1a)–(3.1b) and using the above notation, gives, for $t^{k-1} < t \leq t^k$, $k = 1, \dots, K$, and for all $(\chi, \eta) \in \mathbf{H}^1(\Omega) \times \mathbf{H}_{0|\Gamma_1 \cup \Gamma_2}^1(\Omega)$

$$\begin{aligned} (\partial_t \hat{u}_\tau, \chi) + (\mathbf{A}(\nabla u_\tau^+(t)) \nabla u_\tau^+(t), \nabla \chi) + (g'(u_\tau^+(t)), \chi) \\ = (\mathcal{F}(c_\tau^-(t), u_\tau^-(t), u_\tau^+(t)), \chi) \end{aligned} \quad (4.4a)$$

$$\begin{aligned} (\partial_t \hat{c}_\tau, \chi) + (D(u_\tau^+(t)) \nabla c_\tau^+(t), \nabla \chi) \\ = -(\hat{u}'_\tau(t), \chi) - (D_1(u_\tau^+(t), c_\tau^-(t)) \nabla \phi_\tau^+(t), \nabla \chi) \end{aligned} \quad (4.4b)$$

and

$$(\sigma(u_\tau^+(t)) \nabla \phi_\tau^+(t), \nabla \eta) = -(\hat{u}'_\tau(t) + \sigma'(u_\tau^+(t)) \partial_x u_\tau^+(t), \eta), \quad (4.4c)$$

where

$$\begin{aligned} (\mathcal{F}(c_\tau^-(t), u_\tau^-(t), u_\tau^+(t)), \chi) &:= 30 (m(c_\tau^-) u_\tau^-(t) u_\tau^+(t) (u_\tau^+(t) - 1)^2, \chi) \\ &\quad + 30 ((m(c_\tau^-(t)))^+ (u_\tau^+(t) - 1) u_\tau^+(t) (u_\tau^-(t) - u_\tau^+(t)), \chi). \end{aligned}$$

4.1. Lemma (stability bounds). *Assuming (3.3), we have*

$$\|u_\tau^+\|_{L_\infty([0, T]; L_\infty(\Omega))} + \|u_\tau^+\|_{L_2([0, T]; H^1(\Omega))} + \|\partial_t \hat{u}_\tau\|_{L_2([0, T]; L_2(\Omega))} \leq C, \quad (4.5)$$

$$\|c_\tau^+\|_{L_\infty([0, T]; L_2(\Omega))} + \|c_\tau^+\|_{L_2([0, T]; H^1(\Omega))} + \|\partial_t \hat{c}_\tau\|_{L_2([0, T]; (H^1(\Omega))')} \leq C, \quad (4.6)$$

$$\|\phi_\tau^+\|_{L_2([0, T]; H^1(\Omega))} \leq C. \quad (4.7)$$

Proof. The first and second bounds in (4.5) follow from lemmas 3.2 and 3.5. For the last bound in (4.5), we note from (4.2) that $\partial_t \hat{u}_\tau(t) = d_\tau u^k$ on (t_{k-1}, t_k) , $k = 1, 2, \dots, K$ and thus the result follows from Lemma 3.5.

The bounds in (4.6) and (4.7) follow using similar arguments and the results of lemmas 3.9 and 3.8 respectively. \square

4.2. Lemma (weak compactness). *There exist (u, c, ϕ) and $(\partial_t u, \partial_t c)$ such that for a sequence $(\tau_n)_{n \in \mathbb{N}}$ of positive numbers with $\tau_n \rightarrow 0$ as $n \rightarrow \infty$, we have the following for $1 \leq p < \infty$ if $\dim \Omega = 2$ and $1 \leq p < 6$ if $\dim \Omega = 3$, up to a subsequence, which for simplicity of presentation we again denote by τ_n ,*

$$\hat{u}_{\tau_n}, u_{\tau_n}^{\pm} \xrightarrow{*} u \text{ in } L_{\infty}([0, T]; L_{\infty}(\Omega)), \quad (4.8a)$$

$$\hat{u}_{\tau_n}, u_{\tau_n}^{\pm} \rightharpoonup u \text{ in } L_2([0, T]; H^1(\Omega)), \quad (4.8b)$$

$$\partial_t \hat{u}_{\tau_n} \rightharpoonup \partial_t u \text{ in } L_2([0, T]; L_2(\Omega)), \quad (4.8c)$$

$$\hat{c}_{\tau_n}, c_{\tau_n}^{\pm} \xrightarrow{*} c \text{ in } L_{\infty}([0, T]; L_2(\Omega)), \quad (4.8d)$$

$$\hat{c}_{\tau_n}, c_{\tau_n}^{\pm} \rightharpoonup c \text{ in } L_2([0, T]; H^1(\Omega)), \quad (4.8e)$$

$$\partial_t \hat{c}_{\tau_n} \rightharpoonup \partial_t c \text{ in } L_2([0, T]; (H^1(\Omega))'), \quad (4.8f)$$

$$\phi_{\tau_n}^{\pm} \rightharpoonup \phi \text{ in } L_2([0, T]; H^1(\Omega)), \quad (4.8g)$$

$$u_{\tau_n}^{\pm} \rightarrow u \text{ in } L_2([0, T]; L_p(\Omega)), \quad (4.8h)$$

$$c_{\tau_n}^{\pm} \rightarrow c \text{ in } L_2([0, T]; L_p(\Omega)). \quad (4.8i)$$

Proof. From Lemma 4.1 it follows that there are weakly convergent subsequences that converge to the appropriate limits in (4.8a)-(4.8g). To establish (4.8h) and (4.8i) we use (4.8b), (4.8c), (4.8e), (4.8f) and the Aubin-Lions Lemma [e.g. Roubiřek, 2005]. \square

4.3. Lemma (strong convergence). *For $u \in L_{\infty}([0, T]; L_{\infty}(\Omega))$ and $c \in L_2([0, T]; L_q(\Omega))$, with $1 \leq q < \infty$ if $\dim \Omega = 2$ and $1 \leq q < 3$ if $\dim \Omega = 3$, we have the following, for $1 \leq p < \infty$ if $\dim \Omega = 2$ and $1 \leq p < 6$ if $\dim \Omega = 3$, as $\tau_n \rightarrow 0$*

$$g'(u_{\tau_n}^{\pm}) \rightarrow g'(u) \text{ in } L_2([0, T]; L_p(\Omega)), \quad (4.9a)$$

$$u_{\tau}^{-} u_{\tau}^{+} (u_{\tau}^{+} - 1)^2 \rightarrow u^2 (u - 1)^2 \text{ in } L_2([0, T]; L_p(\Omega)), \quad (4.9b)$$

$$D(u_{\tau_n}^{\pm}) \rightarrow D(u) \text{ in } L_2([0, T]; L_p(\Omega)), \quad (4.9c)$$

$$\sigma(u_{\tau_n}^{\pm}) \rightarrow \sigma(u) \text{ in } L_2([0, T]; L_p(\Omega)), \quad (4.9d)$$

$$m(c_{\tau_n}^{-}) \rightarrow m(c) \text{ in } L_2([0, T]; L_p(\Omega)), \quad (4.9e)$$

$$D_1(u_{\tau_n}^{\pm}, c_{\tau_n}^{-}) \rightarrow D_1(u, c) \text{ in } L_2([0, T]; L_q(\Omega)), \quad (4.9f)$$

$$30m(c_{\tau}^{-})u_{\tau}^{-}u_{\tau}^{+}(u_{\tau}^{+} - 1)^2 \rightarrow m(c)h'(u) \text{ in } L_2([0, T]; L_q(\Omega)), \quad (4.9g)$$

$$(m(c_{\tau}^{-}))^{+}(u_{\tau}^{+} - 1)u_{\tau}^{+}(u_{\tau}^{-} - u_{\tau}^{+}) \rightarrow 0 \text{ in } L_2([0, T]; L_2(\Omega)). \quad (4.9h)$$

Proof. Noting that $g'(u)$, $D(u)$, $\sigma(u)$ are polynomials in u and $m(c)$ is linear in c , the proofs of (4.9a) – (4.9e) follow from Lemma 4.1, (4.8a), (4.8d), (4.8h) and (4.8i). By the triangle inequality, the generalized Hölder inequality with $1/q = 1/p + 1/p'$, (4.6) and (3.9) we obtain

$$\begin{aligned} & \|D(u_{\tau}^{\pm})c_{\tau}^{-} - D(u)c\|_{L_2([0, T]; L_q(\Omega))} \\ &= \|(D(u_{\tau}^{\pm}) - D(u))c_{\tau}^{-} + D(u)(c_{\tau}^{-} - c)\|_{L_2([0, T]; L_q(\Omega))} \\ &\leq \|c_{\tau}^{-}\|_{L_2([0, T]; L_{p'}(\Omega))} \|D(u_{\tau}^{\pm}) - D(u)\|_{L_2([0, T]; L_p(\Omega))} \\ &\quad + \|D(u)\|_{L_2([0, T]; L_{p'}(\Omega))} \|c_{\tau}^{-} - c\|_{L_2([0, T]; L_p(\Omega))} \\ &\leq C(\|D(u_{\tau}^{\pm}) - D(u)\|_{L_2([0, T]; L_p(\Omega))} + \|c_{\tau}^{-} - c\|_{L_2([0, T]; L_p(\Omega))}) \end{aligned} \quad (4.10)$$

and (4.9f) then follows by noting the definition of $D_1(u, c)$ in (2.10), and using (4.9c) and (4.8i). Adopting similar techniques and noting from (2.12) that $h'(u) = 30u^2(u - 1)^2$, from (3.11), (4.5), (4.9b) and (4.9e) we conclude (4.9g).

Noting from (4.2) that $\tau \partial_t \hat{u}_\tau = (u_\tau^- - u_\tau^+)$ for $t \in (t^{k-1}, t^k)$, from (3.11) and (4.5) we have

$$\begin{aligned} \|(m(c_\tau^-)^+ (u_\tau^+ - 1) u_\tau^+ (u_\tau^- - u_\tau^+))\|_{L_2([0, T]; L_2(\Omega))} \\ \leq C \|u_\tau^+ - u_\tau^-\|_{L_2([0, T]; L_2(\Omega))} = C\tau \end{aligned} \quad (4.11)$$

which concludes the proof. \square

4.4. Lemma (weak convergence). For $D(u)\nabla c$, $D_1(u, c)\nabla\phi$, $\sigma(u)\nabla\phi$, $\mathbf{A}(\nabla u)\nabla u \in L_2([0, T]; (L_2(\Omega))^d)$ we have the following as $\tau_n \rightarrow 0$

$$D(u_{\tau_n}^+) \nabla c_{\tau_n}^+ \rightharpoonup D(u)\nabla c \text{ in } L_2([0, T]; (L_2(\Omega))^d), \quad (4.12a)$$

$$D_1(u_{\tau_n}^+, c_{\tau_n}^-) \nabla \phi_{\tau_n}^+ \rightharpoonup D_1(u, c)\nabla\phi \text{ in } L_2([0, T]; (L_2(\Omega))^d), \quad (4.12b)$$

$$\sigma(u_{\tau_n}^+) \nabla \phi_{\tau_n}^+ \rightharpoonup \sigma(u)\nabla\phi \text{ in } L_2([0, T]; (L_2(\Omega))^d), \quad (4.12c)$$

$$\mathbf{A}(\nabla u_{\tau_n}^+) \nabla u_{\tau_n}^+ \rightharpoonup \mathbf{A}(\nabla u)\nabla u \text{ in } L_2([0, T]; (L_2(\Omega))^d). \quad (4.12d)$$

Proof. From Lemma 4.1 we have

$$\begin{aligned} \int_0^T \int_\Omega D(u_{\tau_n}^+) \nabla c_{\tau_n}^+ \cdot \nabla c_{\tau_n}^+ &= \int_0^T \int_\Omega |D^{1/2}(u_{\tau_n}^+) \nabla c_{\tau_n}^+|^2 \\ &\leq \|D^{1/2}(u_{\tau_n}^+) \nabla c_{\tau_n}^+\|_{L_2([0, T]; (L_2(\Omega))^d)}^2 \leq D_{\max} \|c_{\tau_n}^+\|_{L_2([0, T]; H^1(\Omega))}^2 \leq C \end{aligned} \quad (4.13)$$

and hence it follows that there exists a $\xi_1 \in L_2([0, T]; (L_2(\Omega))^d)$ such that

$$D(u_{\tau_n}^+) \nabla c_{\tau_n}^+ \rightharpoonup \xi_1 \text{ in } L_2([0, T]; (L_2(\Omega))^d). \quad (4.14)$$

We now show that $\xi_1 = D(u)\nabla c$, to this end we note that

$$\begin{aligned} &\left| \int_0^T \int_\Omega \left(D(u_{\tau_n}^+) \nabla c_{\tau_n}^+ - D(u)\nabla c \right) \cdot \nabla \psi \right| \\ &= \left| \int_0^T \int_\Omega \left(D(u_{\tau_n}^+) \nabla c_{\tau_n}^+ - D(u)\nabla c_{\tau_n}^+ + D(u)\nabla c_{\tau_n}^+ - D(u)\nabla c \right) \cdot \nabla \psi \right| \\ &\leq \left| \int_0^T \int_\Omega D(u) \left(\nabla c_{\tau_n}^+ - \nabla c \right) \cdot \nabla \psi \right| + \left| \int_0^T \int_\Omega \left(D(u_{\tau_n}^+) - D(u) \right) \nabla c_{\tau_n}^+ \cdot \nabla \psi \right| \\ &\leq \left| \int_0^T \int_\Omega D(u) \left(\nabla c_{\tau_n}^+ - \nabla c \right) \cdot \nabla \psi \right| \\ &\quad + \|D(u_{\tau_n}^+) - D(u)\|_{L_2([0, T]; L_2(\Omega))} \|\nabla c_{\tau_n}^+ \cdot \nabla \psi\|_{L_2([0, T]; L_2(\Omega))}. \end{aligned} \quad (4.15)$$

Since $\|D(u)\|_{L_\infty(\Omega)} \leq C$ from (4.8e), (4.9c) and (4.6) we conclude (4.12a). Using similar techniques we can obtain (4.12b) and (4.12c). We omit the proof of (4.12d) as it is given in [Burman and Rappaz, 2003, Lemma 5.4, p1152]. \square

4.5. Proof of Theorem 2.8. Now we can prove our main result, Theorem 2.8.

Proof. In Theorem 3.1 we established the existence of a solution $(u^k, c^k, \phi^k) \in (H^1(\Omega))^2 \times H_{0|\Gamma_1 \cup \Gamma_2}^1(\Omega)$ of (3.1a)–(3.1c). From lemmas 4.2–4.4 we conclude the existence of a solution $(u, c, \phi) \in (H^1(\Omega))^2 \times H_{0|\Gamma_1 \cup \Gamma_2}^1(\Omega)$ of (2.11a)–(2.11c), with $(u(0), c(0)) = (u_0, c_0) \in H^1(\Omega) \times L_2(\Omega)$ and $u \in L_2([0, T]; H^1(\Omega)) \cap H^1([0, T]; L_2(\Omega)) \cap L_\infty([0, T]; L_\infty(\Omega))$, $c \in L_2([0, T]; H^1(\Omega)) \cap H^1([0, T]; (H^1(\Omega))') \cap L_\infty([0, T]; L_2(\Omega))$ and $\phi \in L_2([0, T]; H_{0|\Gamma_1 \cup \Gamma_2}^1(\Omega))$. \square

5. NUMERICAL SIMULATIONS

In this section we present a finite element discretization of (2.11a)–(2.11c) together with numerical examples that illustrate how dendritic structures can arise from the model.

5.1. Finite element approximation. Until now, for ease of presentation, we have considered a simplified version of the model from Chen et al. [2015] in which, where possible, all physical parameters were set to 1. However in this section, in order to produce computational simulations in which dendritic patterns arise, we consider the original model from Chen et al. [2015] that has the physical parameters reinserted.

As in Section 3, we partition the time interval $[0, T]$ into K equidistant steps, $0 = t_0 < t_1 < \dots < t_{K-1} < t_K = T$, so that for $k = 1, \dots, K$, $t_k := k\tau$. We let \mathcal{T}_h be a regular triangulation of Ω into disjoint open simplices \mathcal{T} and we define $h := \max_{\mathcal{T} \in \mathcal{T}_h} \text{diam } \mathcal{T}$ the maximal element size of \mathcal{T}_h .

Associated with \mathcal{T}_h are the finite element spaces

$$V_h = \{v \in C^0(\bar{\Omega}); v|_{\mathcal{T}} \in P_2(\mathcal{T}), \forall \mathcal{T} \in \mathcal{T}_h\} \subset H^1(\Omega),$$

$$V_{0,h} = \{v \in C^0(\bar{\Omega}); v = 0 \text{ on } \Sigma \subseteq \partial\Omega; v|_{\mathcal{T}} \in P_2(\mathcal{T}), \forall \mathcal{T} \in \mathcal{T}_h\} \subset H^1_{0|\Sigma}(\Omega),$$

where $\Sigma = \Gamma_1 \cup \Gamma_2$ and $P_2(\mathcal{T})$ denotes the set of polynomials of maximum degree 2 on \mathcal{T} .

Using a standard Galerkin finite element method in space and a semi-implicit Euler discretization in time we obtain the following discretisation of a variant of (2.11a)-(2.11c) in which the physical parameters $\epsilon, \gamma, \nu, \mu$ from Chen et al. [2015] have been reinstated, the boundedness imposed on the $D_1(u, c)$, see (2.10), is removed and the electrochemical reaction rate $m(c)$ is replaced with a modified version $\tilde{m}(c)$ to highlight its exponential structure, see [Chen et al., 2015, Appendix B]:

Set $u_h^0 = u_0(\mathbf{x})$ and $c_h^0 = c_0(\mathbf{x})$, then for $k = 1, 2, \dots, K$, given $(u_h^{k-1}, c_h^{k-1}) \in [V_h]^2$ find $(u_h^k, c_h^k, \phi_h^k) \in [V_h]^2 \times V_{0,h}$ such that for all $(\chi_h, \eta_h) \in V_h \times V_{0,h}$

$$\epsilon^2(d_\tau u_h^k, \chi_h) + (\mathbf{A}(\nabla u_h^{k-1}) \nabla u_h^k, \nabla \chi_h) + \gamma(g'(u_h^{k-1}), \chi_h) = (\tilde{m}(c_h^{k-1})h'(u_h^{k-1}), \chi_h), \quad (5.1a)$$

$$(\sigma(u_h^k) \nabla \phi_h^k, \nabla \eta_h) = -\nu(d_\tau u_h^k, \eta_h), \quad (5.1b)$$

$$(d_\tau c_h^k, \chi_h) + (D(u_h^k) \nabla c_h^k, \nabla \chi_h) + (D(u_h^k) c_h^{k-1} \nabla \phi_h^k, \nabla \chi_h) = -\mu(d_\tau u_h^k, \chi_h), \quad (5.1c)$$

where $\tilde{m}(c) = C_1(e^{-C_2} - ce^{C_2})$. The physical parameters are defined, together with their values in the computations, in Table 1. We note that (5.1a) – (5.1c) are linear in u^k , ϕ^k and c^k respectively.

The computational results we present are produced by implementing a standard adaptive strategy, in particular, we use a gradient-based indicator which involves the gradient of the solution of the phase-field equation and the reaction-diffusion equation, given by

$$\eta_{\mathcal{T}} := \sqrt{|\nabla u_h^k|_{\mathcal{T}}^2 + |\nabla c_h^k|_{\mathcal{T}}^2}, \quad (5.2)$$

such that simplices on which $\eta_{\mathcal{T}} \geq 160$ are refined and simplices on which $\eta_{\mathcal{T}} \leq 80$ are coarsened.

5.2. Numerical examples. In this section we present numerical simulations of dendritic crystal growth.

We set $d = 2$ and take $\Omega = [0, 9] \times [-9, 9]$ and $T = 0.5$. For an initial set-up we place a pill-shaped solid seed [cf. Akolkar, 2014, Fig 1] at the mid-point of the left-hand boundary of Ω and set the ion concentration of Li^+ to be 0 along the left hand boundary of Ω , which represents the right most edge of the electrode, and 1 in the remainder of the domain. Thus giving rise to the following initial data for the

order parameter and the concentration:

$$u_0(x_1, x_2) = \begin{cases} 1, & (x_1 - r_0 - \sqrt{r_0^2 - x_2^2})(x_1 + r_0 + \sqrt{r_0^2 - x_2^2})(x_2^2 - r_0^2) \geq 0, \\ 0, & \text{elsewhere.} \end{cases} \quad (5.3)$$

and

$$c_0(x_1, x_2) = \begin{cases} 0, & x_1 = 0, \\ 1, & \text{elsewhere.} \end{cases} \quad (5.4)$$

In the simulations presented below we set $r_0 = 0.1$.

For the implementation of the numerical scheme we used the DUNE Python module, Dedner and Nolte [2018], and the DUNE Alugrid module, Alkämper et al. [2015]. Since the solution is symmetric in the x_2 -direction, for the sake of computational cost, we reduced our computations from the rectangular domain $\Omega = [0, 9] \times [-9, 9]$ to the square domain $\Omega' = [0, 9]^2$. The values of the parameters used in the simulations are presented in Table 1.

We consider the polar form of the anisotropy function (2.15):

$$\tilde{a}(\theta) = a_0(1 + 4\delta \cos(4\theta)), \quad (5.5)$$

with $\theta = \arctan(\partial_{x_2} u / \partial_{x_1} u)$, which yields the anisotropy tensor

$$\mathbf{A}(\theta) = \begin{bmatrix} \tilde{a}^2(\theta) & -\tilde{a}(\theta)\tilde{a}'(\theta) \\ \tilde{a}(\theta)\tilde{a}'(\theta) & \tilde{a}^2(\theta) \end{bmatrix}. \quad (5.6)$$

We present four sets of results, Figure 1 – Figure 4. In Figure 1 we show a simulation of the evolution of a dendritic structure, while in Figures 2 and 3 we examine how the dendritic structure is affected by variations in the anisotropy strength δ and in the parameter μ respectively. In Figure 4 we investigate the effect adding stochastic noise has on the dendritic structure.

Figure 1 depicts the numerical approximations of the order parameter, u_h^k (top row), the concentration of lithium atoms, c_h^k (middle row), and the electrostatic potential, ϕ_h^k (bottom row), each displayed at $t_k = 0.061$ (left) $t_k = 0.244$ (middle) and $t_k = 0.427$ (right). In these results we set $\delta = 0.05$ and $\mu = 2$. From the results for the order parameter we clearly see the formation of a dendritic structure, while a more diffuse form of this structure is mirrored in the concentration results and a very diffuse underlying dendritic structure can also be observed in the electric potential results, with the region, in which $|\phi_h^k|$ attains its maximum value, growing as the dendrite grows, thus eventually causing the battery to fail. When comparing the dendritic structure that forms in Figure 1 to the dendritic structures that are displayed in Figure 4 in Chen et al. [2015] and Figure 3a in Mu et al. [2019] we see that in Figure 1 the structure is smooth and does not form the side branches perpendicular to the growth direction of the dendritic structure, that can be observed in Chen et al. [2015] and Mu et al. [2019]. In Figures 2 and 4 below, we see that dendritic structures with side branches can be observed by increasing the anisotropy strength, δ , or adding stochastic noise.

In Figure 2 we examine how the anisotropy strength, δ , affects the formation of dendritic crystals. To this end we recall the bound $\delta < 1/15 \approx 0.067$ that we impose in assumptions (3.3), recall (3.3), in order for our theoretical results to hold. The specific nature of the bound can be understood from the proof of Lemma 2.5. Figure 2 displays plots of the numerical approximation of the order parameter, u_h^k , at $t_k = 0.366$ for $\mu = 2$ and six values of δ . From this figure we see that the anisotropy strength has a notable impact on the rate at which the dendritic structure grows, in particular the speed of growth increases as δ decreases. In addition, we see that the value $\delta = 1/15 \approx 0.067$ plays a significant role; in the simulations where $\delta \ll 1/15 \approx 0.067$, i.e. Figure 2a – Figure 2d in which $\delta = 0, 0.01, 0.02, 0.05$

respectively, the geometry of the dendritic structure is smooth, while in Figure 2e, where $\delta = 0.065$ and hence the condition $\delta < 1/15$ is only just satisfied, the structure is no longer smooth and small instabilities, perpendicular to the growth of the dendritic structure, have started to form. The instabilities are more pronounced in Figure 2f, which shows $\delta = 0.1$ which is significantly greater than $\delta = 1/15$. $\delta \geq 1/15$, the numerical scheme still produces solutions for values of $\delta > 1/15$.

In Figure 3 we examine how the evolution of the order parameter, u , varies with the parameter μ , which is related to the ratio of site density of Li and the standard bulk concentration of electrolyte solution as described in Chen et al. [2015]. We display plots of the numerical approximation of the order parameter, u_h^k , at $t_k = 0.122$ for $\delta = 0.05$ and five values of μ , together with, for comparison, a plot of u_h^k resulting from solving the system (5.1a)–(5.1c) with $\delta = 0$ and $\mu = 0$. From this figure we see that for small values of μ , i.e. $\mu = 0$ and $\mu = 0.5$, no dendritic structures arise and instead the geometry takes a form that is relatively radially symmetric, while for larger values of μ , namely $\mu = 1, 1.5, 2$ dendritic patterns arise, with the dendritic structure becoming more pronounced, yet growing more slowly, as μ increases.

As observed above, in Figure 1 no side branches are formed perpendicular to the growth direction of the dendritic structure, whereas in the results in Chen et al. [2015] and Mu et al. [2019] side branches do form. From Figure 2 we see that side branches are observed if the anisotropy strength, δ , is taken large enough. An alternative approach to yield the formation of side branches is to add stochastic noise to the model, to this end we follow the authors in Kobayashi [1993] and add a stochastic term, $\beta u_h^k(1 - u_h^k)X$, to (5.1a), so that it becomes

$$\begin{aligned} \epsilon^2(d_\tau u_h^k, \chi_h) + (\mathbf{A}(\nabla u_h^{k-1})\nabla u_h^k, \nabla \chi_h) + \gamma(g'(u_h^{k-1}), \chi_h) = & (\tilde{m}(c_h^{k-1})h'(u_h^{k-1}), \chi_h) \\ & - (\beta u_h^k(1 - u_h^k)X, \chi_h), \quad \forall \chi_h \in V_h, \end{aligned} \quad (5.7)$$

where $X \sim \mathcal{U}(-1/2, 1/2)$ and $\beta > 0$ is a scalar that controls the noise strength. Results obtained from the model with (5.1a) replaced by (5.7), and $\delta = 0.05$ and $\mu = 2$, are shown in Figure 4, which displays plots of the numerical approximation of the order parameter, u_h^k , at $t_k = 0.305$ for four values of β . From this figure we see that when $\beta = 0.03$ side branches have started to form and that the length of these branches increases as β increases.

TABLE 1. Dimensionless parameters.

Parameter	Notation	Value
Diffusion coefficient in the electrolyte	D^e	3.0
Diffusion coefficient in the electrode	D^s	2.5
Conductivity coefficient in the electrolyte	σ^e	100.0
Conductivity coefficient in the electrode	σ^s	10^7
Interfacial mobility	γ	1.0
Characteristic time scale	ϵ^2	0.0003
Anisotropy strength	δ	0.05 (unless otherwise specified)
Interfacial thickness	a_0	0.01
Electrochemical reaction rate coefficients	C_1 & C_2	1/15 & 1.9345
Coefficient multiplying $d_\tau u_h^k$ in (5.1b)	ν	76.4
Coefficient multiplying $d_\tau u_h^k$ in (5.1c)	μ	2.0 (unless otherwise specified)

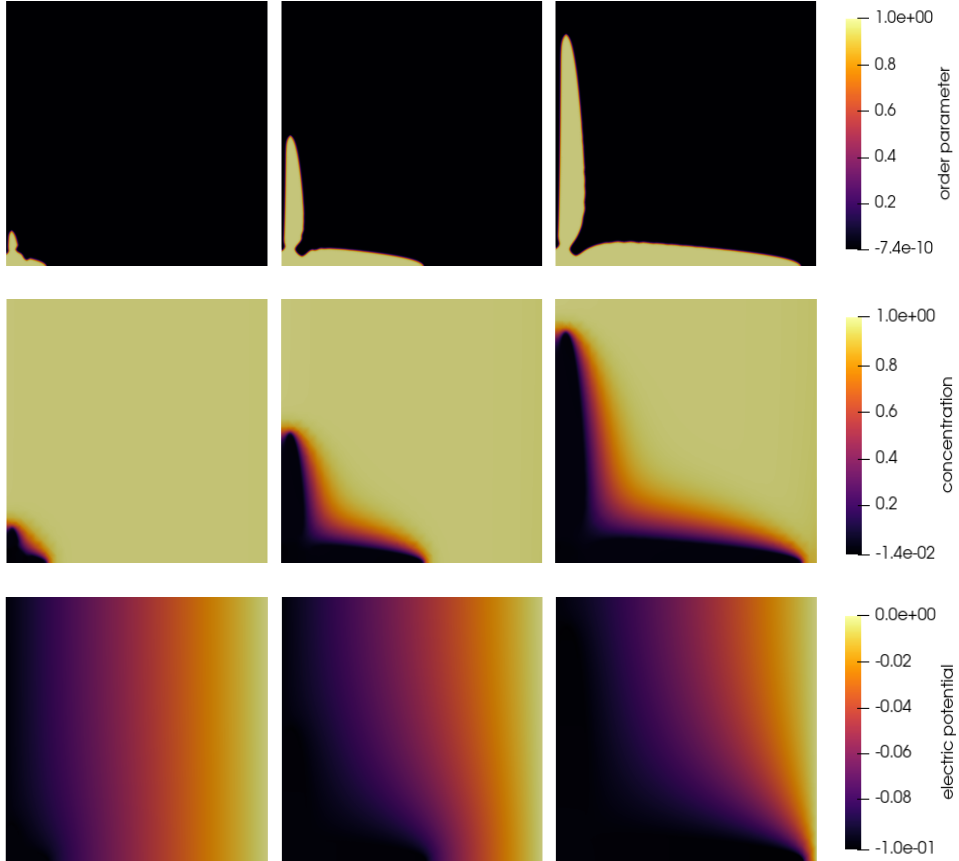


FIGURE 1. Dendritic formation with $\delta = 0.05$ and $\mu = 2$: u_h^k (top row), c_h^k (middle row) and ϕ_h^k (bottom row) displayed at $t_k = 0.061$ (left) $t_k = 0.244$ (middle) and $t_k = 0.427$ (right)

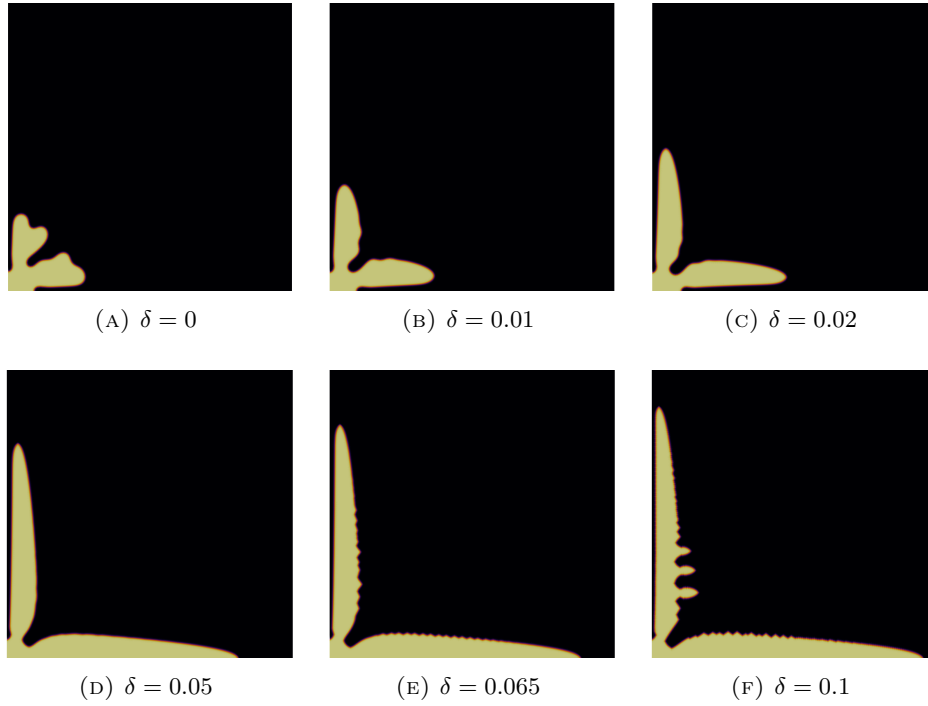


FIGURE 2. Comparison of u_h^k at $t_k = 0.366$ with $\mu = 2$ and different values for the anisotropy strength δ , introduced in (2.15).

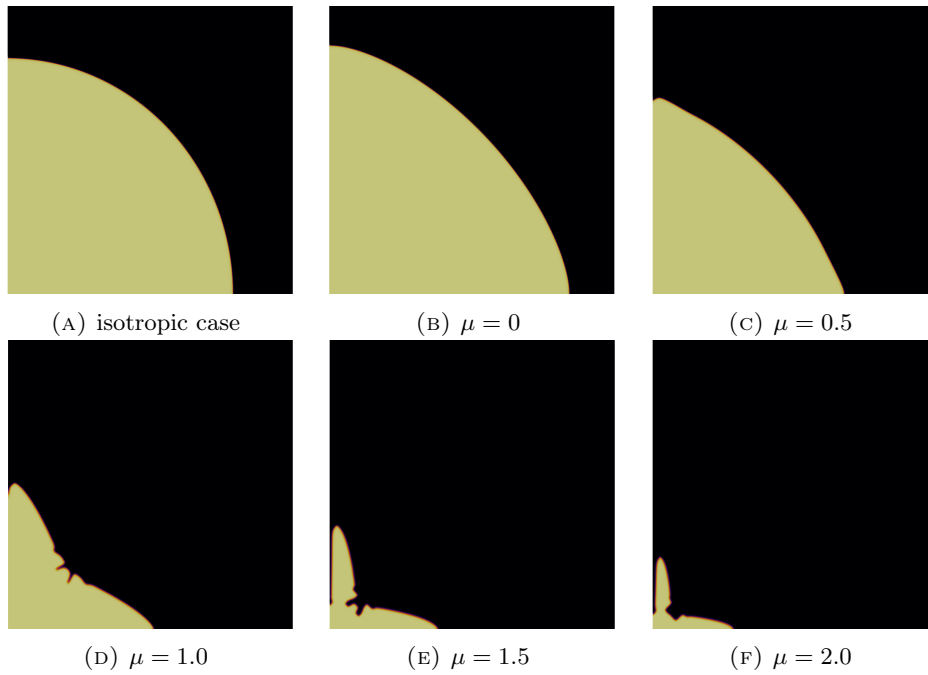


FIGURE 3. Comparison of u_h^k at $t_k = 0.122$ with $\delta = 0.05$ for different values of μ .

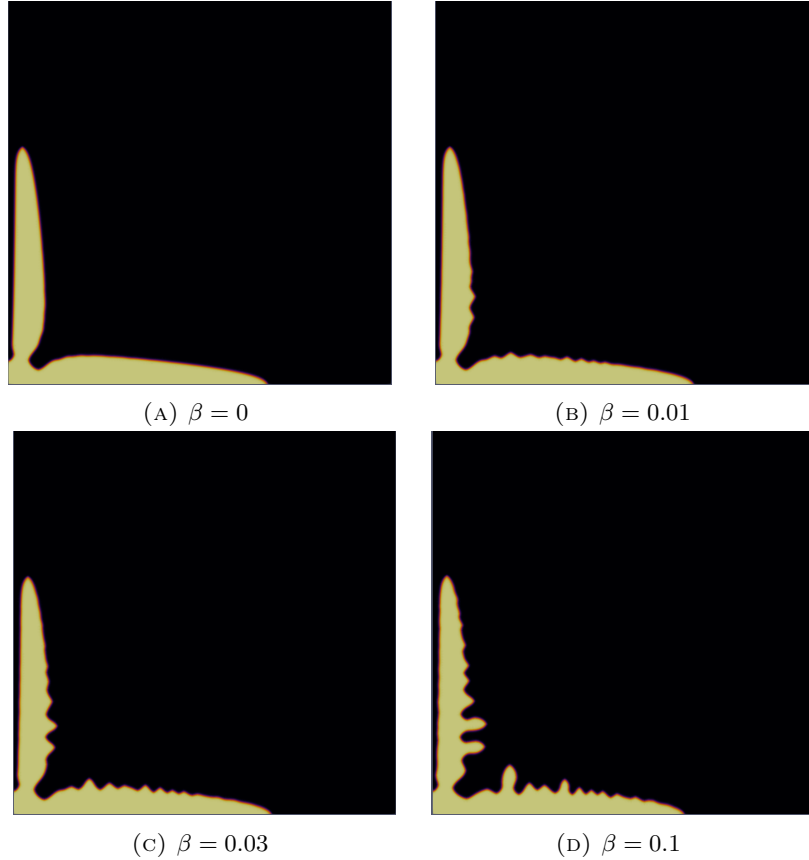


FIGURE 4. Comparison of u_h^k at $t_k = 0.305$ with $\delta = 0.05$ and $\mu = 2$, for solutions to the model with (5.1a) replaced by (5.7) for different values of the noise amplitude β .

ACKNOWLEDGEMENTS

AS was partially funded by the European Union (ERC Synergy, NEMESIS, project number 101115663).

Views and opinions expressed are however those of the authors only and do not necessarily reflect those of the European Union or the European Research Council Executive Agency. Neither the European Union nor the granting authority can be held responsible for them.

OL and VS were partly supported in this work by the Dr Perry James (Jim) Browne Research Centre on Mathematics and its Applications at the University of Sussex, UK.

REFERENCES

- R. Akolkar. Mathematical model of the dendritic growth during lithium electrodeposition. *Journal of Power Sources*, 232:23–28, 06 2013. ISSN 03787753. doi:10.1016/j.jpowsour.2013.01.014. URL <https://linkinghub.elsevier.com/retrieve/pii/S0378775313000323>.
- R. Akolkar. Modeling dendrite growth during lithium electrodeposition at sub-ambient temperature. *Journal of Power Sources*, 246:84–89, 01 2014. ISSN 03787753. doi:10.1016/j.jpowsour.2013.07.056. URL <https://linkinghub.elsevier.com/retrieve/pii/S0378775313012469>.

- M. Alkämper, A. Dedner, R. Klöfkorn, and M. Nolte. The DUNE-ALUGrid Module. Technical report, arXiv, 08 2015. URL <http://arxiv.org/abs/1407.6954>.
- S. Bartels. *Numerical Methods for Nonlinear Partial Differential Equations*, volume 47 of *Springer Series in Computational Mathematics*. Springer International Publishing, 2015. ISBN 978-3-319-13796-4 978-3-319-13797-1. doi:10.1007/978-3-319-13797-1. URL <http://link.springer.com/10.1007/978-3-319-13797-1>.
- E. Burman and J. Rappaz. Existence of solutions to an anisotropic phase-field model. *Mathematical Methods in the Applied Sciences*, 26(13):1137–1160, 09 2003. ISSN 0170-4214, 1099-1476. doi:10.1002/mma.405. URL <https://onlinelibrary.wiley.com/doi/10.1002/mma.405>.
- L. Chen, H. W. Zhang, L. Y. Liang, Z. Liu, Y. Qi, P. Lu, J. Chen, and L.-Q. Chen. Modulation of dendritic patterns during electrodeposition: A nonlinear phase-field model. *Journal of Power Sources*, 300:376–385, 2015. ISSN 03787753. doi:10.1016/j.jpowsour.2015.09.055. URL <https://linkinghub.elsevier.com/retrieve/pii/S0378775315303141>.
- B. Dacorogna. *Direct Methods in the Calculus of Variations*. Number v. 78 in Applied Mathematical Sciences. Springer, 2nd ed edition, 2008. ISBN 978-0-387-35779-9 978-0-387-55249-1.
- A. Dedner and M. Nolte. The Dune Python Module. Technical report, arXiv, 07 2018. URL <http://arxiv.org/abs/1807.05252>.
- C. M. Elliott and R. Schätzle. The limit of the anisotropic double-obstacle Allen–Cahn equation. *Proceedings of the Royal Society of Edinburgh: Section A Mathematics*, 126(6):1217–1234, 1996. ISSN 0308-2105, 1473-7124. doi:10.1017/S0308210500023374. URL https://www.cambridge.org/core/product/identifiser/S0308210500023374/type/journal_article.
- C. M. Elliott and R. Schätzle. The Limit of the Fully Anisotropic Double-Obstacle Allen–Cahn Equation in the Nonsmooth Case. *SIAM Journal on Mathematical Analysis*, 28(2):274–303, 03 1997. ISSN 0036-1410, 1095-7154. doi:10.1137/S0036141095286733. URL <http://epubs.siam.org/doi/10.1137/S0036141095286733>.
- L. C. Evans. *Partial Differential Equations*. Number v. 19 in Graduate Studies in Mathematics. American Mathematical Society, 1998. ISBN 978-0-8218-0772-9.
- C. Gräser. *Convex Minimization and Phase Field Models*. PhD thesis, Freie Universität Berlin, Berlin, DE, 2011. URL https://refubium.fu-berlin.de/bitstream/fub188/7385/1/c_graeser_dissertation.pdf.
- C. Graser, R. Kornhuber, and U. Sack. Time discretizations of anisotropic Allen–Cahn equations. *IMA Journal of Numerical Analysis*, 33(4):1226–1244, 10 2013. ISSN 0272-4979, 1464-3642. doi:10.1093/imanum/drs043. URL <https://academic.oup.com/imajna/article-lookup/doi/10.1093/imanum/drs043>.
- J. E. Guyer, W. J. Boettinger, J. A. Warren, and G. B. McFadden. Model of Electrochemical "Double Layer" Using the Phase Field Method. Technical report, arXiv, 03 2002. URL <http://arxiv.org/abs/cond-mat/0203420>.
- J. E. Guyer, W. J. Boettinger, J. A. Warren, and G. B. McFadden. Phase field modeling of electrochemistry II: Kinetics. *Physical Review E*, 69(2):021604, 02 2004a. ISSN 1539-3755, 1550-2376. doi:10.1103/PhysRevE.69.021604. URL <http://arxiv.org/abs/cond-mat/0308179>.
- J. E. Guyer, W. J. Boettinger, J. A. Warren, and G. B. McFadden. Phase field modeling of electrochemistry I: Equilibrium. *Physical Review E*, 69(2):021603, 02 2004b. ISSN 1539-3755, 1550-2376. doi:10.1103/PhysRevE.69.021603. URL <http://arxiv.org/abs/cond-mat/0308173>.

- A. Karma and W.-J. Rappel. Quantitative phase-field modeling of dendritic growth in two and three dimensions. *Physical Review E*, 57(4):4323–4349, 04 1998. ISSN 1063-651X, 1095-3787. doi:10.1103/PhysRevE.57.4323. URL <https://link.aps.org/doi/10.1103/PhysRevE.57.4323>.
- R. Kobayashi. Modeling and numerical simulations of dendritic crystal growth. *Physica D: Nonlinear Phenomena*, 63(3-4):410–423, 03 1993. ISSN 01672789. doi:10.1016/0167-2789(93)90120-P. URL <https://linkinghub.elsevier.com/retrieve/pii/016727899390120P>.
- R. Kobayashi. A Numerical Approach to Three-Dimensional Dendritic Solidification. *Experimental Mathematics*, 3(1):59–81, 01 1994. ISSN 1058-6458, 1944-950X. doi:10.1080/10586458.1994.10504577. URL <http://www.tandfonline.com/doi/abs/10.1080/10586458.1994.10504577>.
- L. Liang and L.-Q. Chen. Nonlinear phase field model for electrodeposition in electrochemical systems. *Applied Physics Letters*, 105(26):263903, 12 2014. ISSN 0003-6951, 1077-3118. doi:10.1063/1.4905341. URL <http://aip.scitation.org/doi/10.1063/1.4905341>.
- L. Liang, Y. Qi, F. Xue, S. Bhattacharya, S. J. Harris, and L.-Q. Chen. Nonlinear phase-field model for electrode-electrolyte interface evolution. *Physical Review E*, 86(5):051609, 11 2012. ISSN 1539-3755, 1550-2376. doi:10.1103/PhysRevE.86.051609. URL <https://link.aps.org/doi/10.1103/PhysRevE.86.051609>.
- G. B. McFadden, A. A. Wheeler, R. J. Braun, S. R. Coriell, and R. F. Sekerka. Phase-field models for anisotropic interfaces. *Physical Review E*, 48(3):2016–2024, 09 1993. ISSN 1063-651X, 1095-3787. doi:10.1103/PhysRevE.48.2016. URL <https://link.aps.org/doi/10.1103/PhysRevE.48.2016>.
- W. Mu, X. Liu, Z. Wen, and L. Liu. Numerical simulation of the factors affecting the growth of lithium dendrites. *Journal of Energy Storage*, 26:100921, 12 2019. ISSN 2352152X. doi:10.1016/j.est.2019.100921. URL <https://linkinghub.elsevier.com/retrieve/pii/S2352152X19304268>.
- Y. Okajima, Y. Shibuta, and T. Suzuki. A phase-field model for electrode reactions with Butler–Volmer kinetics. *Computational Materials Science*, 50(1):118–124, 2010. ISSN 09270256. doi:10.1016/j.commatsci.2010.07.015. URL <https://linkinghub.elsevier.com/retrieve/pii/S0927025610004337>.
- T. Roubiček. *Nonlinear Partial Differential Equations with Applications*. Number v. 153 in International Series of Numerical Mathematics. Birkhäuser Verlag, 2005. ISBN 978-3-7643-7293-4.
- R. Showalter. *Monotone Operators in Banach Space and Nonlinear Partial Differential Equations*, volume 49 of *Mathematical Surveys and Monographs*. American Mathematical Society, 02 2013. ISBN 978-0-8218-9397-5 978-1-4704-1280-7. doi:10.1090/surv/049. URL <http://www.ams.org/surv/049>.
- J. E. Taylor and J. W. Cahn. Diffuse interfaces with sharp corners and facets: Phase field models with strongly anisotropic surfaces. *Physica D: Nonlinear Phenomena*, 112(3-4):381–411, 02 1998. ISSN 01672789. doi:10.1016/S0167-2789(97)00177-2. URL <https://linkinghub.elsevier.com/retrieve/pii/S0167278997001772>.
- A. A. Wheeler and G. B. McFadden. A xi-vector formulation of anisotropic phase-field models: 3D asymptotics. *European Journal of Applied Mathematics*, 7(4):367–381, 08 1996. ISSN 0956-7925, 1469-4425. doi:10.1017/S0956792500002424. URL https://www.cambridge.org/core/product/identifier/S0956792500002424/type/journal_article.
- Wolfram Research, Inc. Mathematica, 2024. URL <https://www.wolfram.com/mathematica>.

V. Yurkiv, T. Foroozan, A. Ramasubramanian, R. Shahbazian-Yassar, and F. Mashayek. Phase-field modeling of solid electrolyte interface (SEI) influence on Li dendritic behavior. *Electrochimica Acta*, 265:609–619, 03 2018. ISSN 00134686. doi:10.1016/j.electacta.2018.01.212. URL <https://linkinghub.elsevier.com/retrieve/pii/S0013468618302809>.

INSTITUT MONTPELLIÉRAIN ALEXANDER GROTHENDIECK, UNIVERSITÉ DE MONTPELLIER, FRANCE
Email address: `alskouras@gmail.com`

DEPARTMENT OF MATHEMATICS, UNIVERSITY OF SUSSEX, BRIGHTON UK
Email address: `lakkis.o.math@gmail.com`

DEPARTMENT OF MATHEMATICS, UNIVERSITY OF SUSSEX, BRIGHTON UK
Email address: `v.styles@sussex.ac.uk`